ELSEVIER

Coordination Chemistry Reviews 143 (1995)
611–636

COORDINATION CHEMISTRY REVIEWS

Polyicosahedricity: icosahedron to icosahedron of icosahedra growth pathway for bimetallic (Au—Ag) and trimetallic (Au—Ag—M; M = Pt, Pd, Ni) supraclusters; synthetic strategies, site preference, and stereochemical principles

Boon K. Teo, Hong Zhang

Department of Chemistry, Room 4500, University of Illinois at Chicago, 845 W. Taylor Street, Chicago, IL 60607, USA

Received 30 November 1994

Contents

Abstract

In this review, syntheses and structural systematics of a series of vertex-sharing polyicosahedral clusters containing group 11 (Au,Ag,Cu) and group 10 (Pt,Pd,Ni) metals are discussed.

SSDI 0010-8545(95)01136-6

This particular series of clusters follows a well-defined growth pathway in which the basic building block is the 13-atom centered icosahedron. The design rule is vertex sharing and the cluster "grows" by successive additions of icosahedral units via sharing of atoms. This cluster of clusters growth mechanism from a single icosahedron (13 atoms) to an icosahedron of icosahedra (127 atoms) parallels the atom-by-atom growth from a single atom to a 13-atom icosahedron and hence may be considered as a manifestation of the spontaneous self-organization and self-similarity aggregation process in the early stages of particle growth. This tendency to form polyicosahedral clusters may be termed polyicosahedricity. Recent developments in synthetic strategies and stereochemical principles of bi- and trimetallic vertex-sharing polyicosahedral clusters are highlighted with emphasis on (1) *endo* icosahedral chemistry by incorporating group 10 metals in the centers of the icosahedra, (2) *exo* icosahedral chemistry by capping the icosahedral faces with metal atoms or by "capturing" small molecules in the cluster cavities, and (3) framework icosahedral chemistry by changing the metal combination (group 11 metals) of the cluster architecture. Specifically, a new synthetic strategy based on "preformed clusters", site preference rules, new concepts such as rotamerism and roulettamerism, and a new intracavity chemistry on a cluster surface resembling Venus flytrap are discussed. It is hoped that basic understanding of the stereochemical and bonding principles governing alloy formation in multimetallic clusters will lead to better electronic and stereochemical controls of their structures and reactivities and, ultimately, give rise to better design and manufacture or fabrication of structurally well-defined and functionally optimized nanoarchitecture, multimetallic catalysts, etc.

Keywords: Polyicosahedricity; Supraclusters; Icosahedra

Introduction: scope and significance

An icosahedron has 12 vertices, 20 triangular faces, and 30 edges. It conforms to the icosahedral point group, I_h, which has 120 symmetry operations, the highest possible in three dimensions (the only exception is the spherical harmonics point group K_h; see, for example, Ref. [1]). The last decade has seen an unusual surge of research activities in cluster chemistry involving the icosahedron [2–11]. The recent syntheses and structural determinations of metal carbonyl clusters have also resulted in a variety of discrete icosahedral clusters containing transition metals and main group elements [4–8]. Furthermore, the icosahedron has emerged as a basic unit in solid state materials such as several allotropes of boron [12], complex borides [13], gallides [14], and quasi-crystalline aluminum alloys [15].

Icosahedral geometry is particularly favored by "electron-deficient" clusters [2,3,9–12] in which the electron counts are insufficient to form two-center two-electron bonds. A complete triangulation of the polyhedral cluster surface such as that of an icosahedron implies a maximization of the number of bonding interactions between atoms, thus providing extra (energetic) stability for the cluster. For example, boron-containing [2,3,12] and gold-containing [9–11] clusters are often based on non-centered and centered icosahedra as portrayed in Figs. 1(a) and 1(b) respectively,

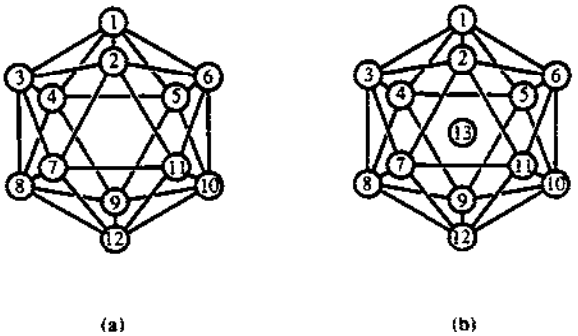

Fig. 1. (a) Non-centered icosahedron; (b) centered icosahedron.

both as a result of their low electron counts. In the case of gold clusters, the low electron counts can be attributed to the relativistic effects [17].

High nuclearity mixed-metal clusters are important in that they may serve as structurally well-defined models for multimetallic catalysts or nanoparticles [4–11,16,18–21]. Our ongoing work in this area has given rise to a unique series of vertex-sharing polyicosahedral clusters containing group 11 (Au,Ag,Cu) and group 10 (Pt,Pd,Ni) metals [11,22–26]. The first three members of the sequence are depicted in Fig. 2. This particular series of clusters follows a well-defined growth pathway in which the basic building block is the 13-atom icosahedron (Fig. 2(a)). The design rule is vertex sharing and the cluster "grows" by successive additions of icosahedral units via sharing of atoms. We refer to these high nuclearity mixed-metal clusters as

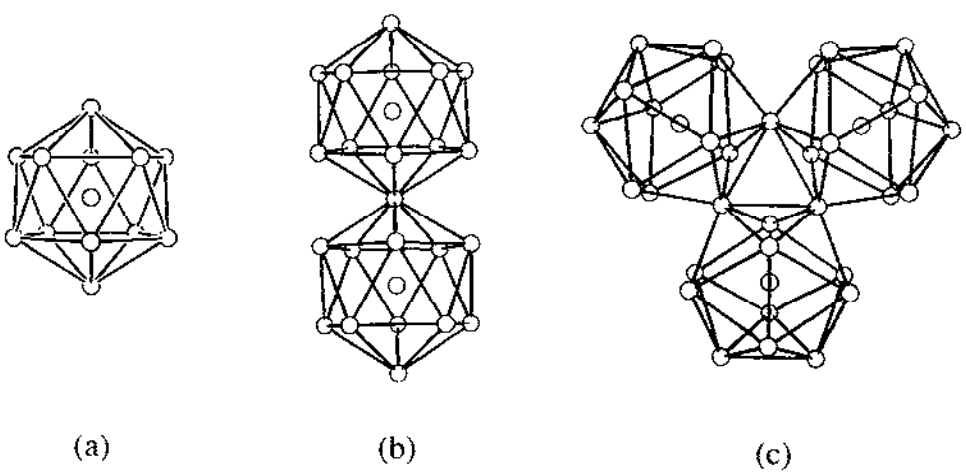

Fig. 2. The first three members of vertex-sharing polyicosahedral supraclusters: (a) icosahedron; (b) biicosahedra; (c) triicosahedra.

"clusters of clusters" [11,22–26]. This "cluster of clusters" concept allows us to envisage, design, and build large cluster assemblies in the nanorealm.

The most important characteristics of this particular series of clusters of clusters are its precise design rule and growth sequence. This cluster of clusters growth mechanism from a single icosahedron (13 atoms) to an icosahedron of icosahedra (127 atoms) parallels the atom-by-atom growth pathway for the primary clusters from a single atom to a 13-atom icosahedron, as depicted in Fig. 3. This tendency of forming polyicosahedral cluster framework may be termed "polyicosahedricity". Many examples are known, e.g. the biicosahedral [11a–11g], the triicosahedral [11h–11k], and the tetraicosahedral clusters [11l]. We believe that this "cluster of clusters" sequence is a manifestation of the spontaneous self-organization and self-similarity aggregation process in cluster growth [22a]. Such growth mechanism, and

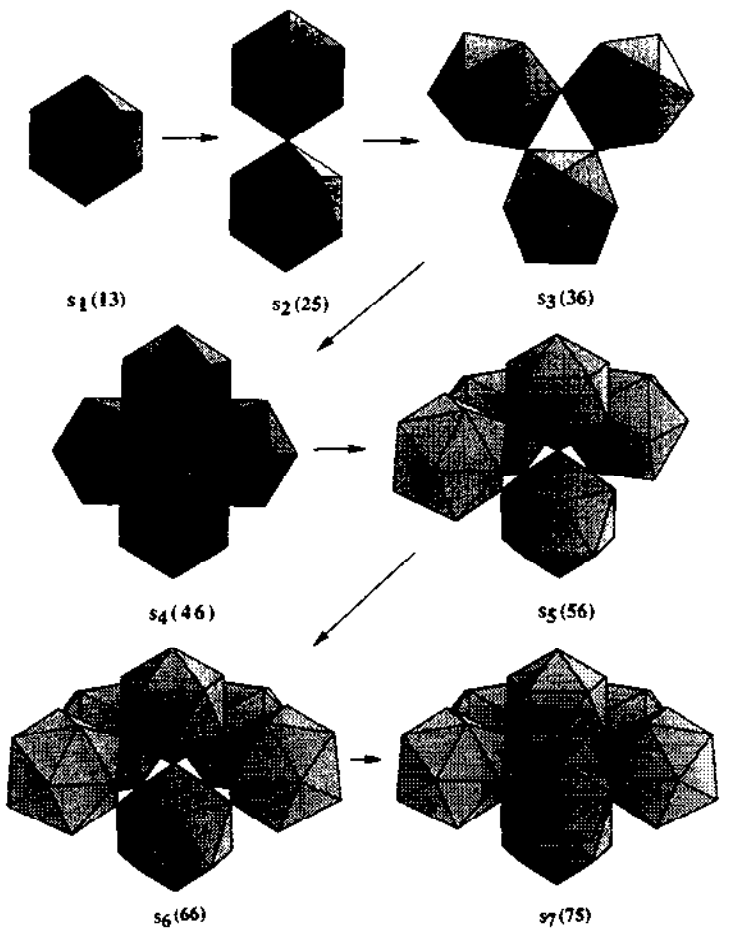

Fig. 3.

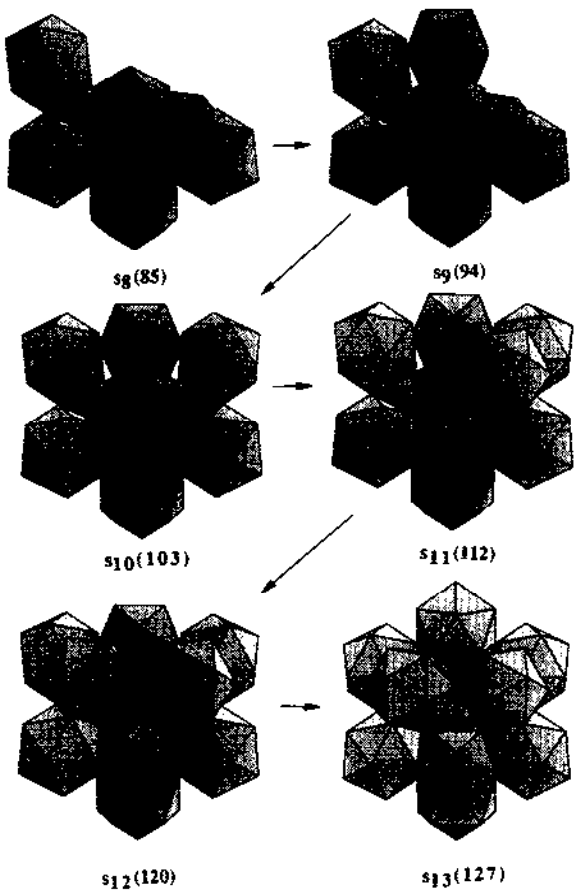

Fig. 3 (continued). Polyicosahedricity: vertex-sharing polyicosahedral growth sequence, $s_n(N)$, from an icosahedron to an icosahedron of icosahedra, where n is the number of icosahedra and N is the overall nuclearity.

the resulting geometry and symmetry, is fractal [27] in character which is quite common in nature. Furthermore, the formation and growth of these clusters, as elucidated by their structures in a stepwise manner, may represent "snapshots" of the early stages of the nucleation and growth of ultrafine metal particles.

In this review, we wish to further develop the cluster of clusters (building block) approach to large metal clusters by (1) designing and building novel and larger cluster assemblies via a new synthetic strategy based on "preformed clusters", (2) understanding and controlling alloy formation by employing a variety of metal and ligand combinations, and (3) discovering new stereochemical or bonding principles governing their structures and bonding. Specific metal and/or ligand combinations are chosen for the syntheses of particular target molecules in order to build new cluster assemblies, to test certain hypotheses, or to develop new concepts. It is

hoped that this research will not only shed light on the nucleation and growth of fine particles, quasi-crystals, and amorphous materials but also lead to new cluster compounds with unusual properties of relevance to critical technologies such as nanostructures [28] and catalysis [29]. Understanding of the stereochemical and bonding principles governing site preference in heteronuclear metal clusters will lead to better electronic and stereochemical controls of their structures and reactivities. Ultimately, such information will result in a detailed understanding of alloy formation in multimetallic systems or phases and in better design and the manufacture or fabrication of structurally well-defined and functionally optimized multimetallic catalysts, ultrafine particles, nanoarchitectures, quantum devices etc.

2. Synthetic strategies

2.1. Metal frameworks

2.1.1. Vertex-sharing polyicosahedral cluster growth via reductive condensation

Our most successful synthetic route to these supraclusters (s_n) (cf. Fig. 3) is based on a spontaneous but stepwise agglomeration of smaller cluster units via progressive reduction. This reductive condensation has proved to be a viable approach to large metal clusters as evidenced by the successful syntheses and structures of the polyicosahedral metal cluster series in our laboratory [11,22–26].

We have also demonstrated spectroscopically [30] that the s_n (nuclearity) supraclusters are indeed formed in a stepwise manner with progressive reduction (where R represents the reductant) as follows:

$$M^{1+} \xrightarrow{R} s_1(13) \xrightarrow{R} s_2(25) \xrightarrow{R} s_3(36) \xrightarrow{R} s_4(46) \cdots \xrightarrow{R} s_{13}(127)$$

In other words, instead of adding one atom at a time, the cluster "grows" by adding one icosahedron at a time (cf. Fig. 3), giving rise to a well-defined growth sequence (i.e. based on vertex-sharing icosahedra).

2.1.2. Building cluster assemblies via preformed clusters as building blocks

Until recently, we have focused our primary attention on the Au—Ag system. While gold and silver have proven to be a good combination in the presence of phosphine and halide ligands, other intriguing mixed-metal clusters have been synthesized and structurally characterized by several research groups. For example, several highly interesting Pt—Au and Pt—Au—Ag clusters have been reported by Pignolet, Steggerda, and coworkers [21], e.g. $[PtAu_6(PPh_3)_7]^{2+}$, $[PtAu_7(PPh_3)_8H]^{2+}$, $[PtAu_8(PPh_3)_8]^{2+}$, $[PtAu_8(PPh_3)_8(CO)]^{2+}$, $[PtAgAu_8(PPh_3)_8]^{3+}$, $[PtAgAu_8(PPh_3)_8(CO)]^{3+}$. These clusters can be used as preformed building blocks in synthesizing the polyicosahedral series. Indeed, we have recently synthesized the first examples of trimetallic clusters containing group 10 and 11 metals, e.g. $[(Ph_3P)_{10}Au_{12}Ag_{12}MCl_7]^+$ [25] and $[(Ph_3P)_{10}Au_{11}Ag_{12}M_2Cl_7]$ [26], where

M = Pt, Pd, Ni, via this new synthetic strategy (reductive addition of a third metal to a preformed bimetallic cluster):

$$[(Ph_3P)_8Au_8M]^{2+} + [(Ph_3P)AgCl]_4 \xrightarrow{NaBH_4} [(Ph_3P)_{10}Au_{12}Ag_{12}MCl_7]^{-}$$

$$+ [(Ph_3P)_{10}Au_{11}Ag_{12}M_2Cl_7]$$

where M = Pt, Pd, Ni

A similar cluster $[(Ph_3P)_{10}Au_{10}Ag_{13}Pt_2Cl_7]$, which has a shared Ag vertex (instead of Au), has also been synthesized by Steggerda and coworkers [31]. These new clusters open the door to other interesting trimetallic Au—Ag—M clusters (where M = group 10 metals). We hope to synthesize the parallel sequence (Fig. 3) of trimetallic (Au—Ag—M where M is a group 10 metal) vertex-sharing polyicosahedral supraclusters, from a single icosahedron of 13 metal atoms to an icosahedron of icosahedra of 127 metal atoms, in analogy to the bimetallic (Au—Ag) vertex-sharing polyicosahedral clusters [11,22–26], via this new synthetic route.

2.2. *Ligand environment: steric and electronic controls*

To date, a wide variety of ligands have been investigated by us with the hope of understanding the steric and electronic effects of the ligands on the metal frameworks:

2.2.1. *Steric effects*

While *p*-tol_3P and Ph_3P differ little in their metal bonding capabilities, the observed structural changes are nontrivial (vide infra). We have, therefore, investigated the effect of the sterically more demanding ligands such as *o*- and *m*-tol_3P on the structure. Repeated attempts to isolate the same Au—Ag cluster series by using *o*-tol_3P have been unsuccessful to date (as a result, presumably, of much greater steric repulsions between the *ortho*-methyl group and the metal atoms). On the contrary, *m*-tol_3P gives rise to an interesting series of cluster compounds which are currently under study. For example, $[(m\text{-}tol_3P)_{10}Au_{13}Ag_{12}Cl_8]^{-}$ adopts a biicosahedral structure which is distinctly different from *p*-tol_3P or Ph_3P. Details will be published elsewhere [32a].

2.2.2. *Electronic effects*

How will the molecular architecture change if we change the electron donating or withdrawing power of the phosphine ligands? One way is to put an electron-donating or an electron-withdrawing group on the phenyl groups of the phosphines. To minimize the steric effect which is addressed separately above, we chose to use *para*-substituted Ph_3P ligands. It is customary to subdivide the electron-donating (+) or withdrawing (−) power of the substituents as inductive (I) and resonance (M) effects. In this context, CH_3 is electron-donating on both counts (i.e. +I and +M), OCH_3 and Cl are −I and +M, and NO_2 and COOR are −I and −M. For example, the recently synthesized cluster, $[\{p\text{-}CH_3OC_6H_4\}_3P\}_{10}Au_{13}Ag_{12}Cl_8]^{+}$ [32b] has an

interesting metal core configuration and an unusual ligand arrangement. This cluster is also interesting in that it has an extensive network of hydrogen bonding. Details can be found elsewhere [30]. Plans are underway to investigate the effects of other substituents such as i-Pr, *t*-Bu, NMe_2, $N(i\text{-}Pr)_2$, $CONR_2$, COOR on the cluster structure.

3. Site preference and alloy formation

Site preference in mixed-metal clusters is a manifestation of the various and often competing bonding effects. The interrelations and interplay of these structural and bonding effects have profound influence on alloy formation in materials such as multimetallic catalysts [29], nanoparticles [28], thin films or surfaces [33] etc. Understanding of such alloy formation will allow better electronic and stereochemical controls of their structures and hence improve the design and manufacture of these materials (e.g. preparation of well-defined catalysts with tailor-made reactivities and selectivities or fabrication of quantum devices with specific functions).

3.1. Site preference principles in multimetallic polyicosahedral supraclusters

We shall use the bi- and trimetallic vertex-sharing biicosahedral cluster sequences, depicted in Table 2, to illustrate the site preference principles in multimetallic polyicosahedral clusters. The site preference rules are summarized in Table 1.

3.1.1. Bimetallic Au—Ag supraclusters

For the bimetallic polyicosahedral Au—Ag supraclusters [11,22–26], six empirical structural rules have been established (Table 1) [11k]: (1) the centers of the icosahedra are gold atoms; (2) the "shared" vertices are most likely to be gold atoms (but with some exceptions); (3) phosphine ligands prefer coordination with surface gold atoms (with some exceptions); (4) silver atoms prefer surface sites, especially those at the boundary of neighboring icosahedra; (5) the capping atoms are most likley to be silver atoms; (6) halide ligands prefer coordination with silver atoms. As

Table 1
Site preference for trimetallic vertex-sharing biicosahedral supraclusters containing group 10 and 11 metals

	Site preference
Center	Ni, Pd, Pt > Au
	∨
Vertex	Au > Ag
	∨ ∧
Surface P	Au > Ag
	∨ ∧
Surface X	Au < Ag

pointed out previously [11k,24], these structural rules can be rationalized in terms of the disparities in metal–metal and metal–ligand interactions, as well as in electronegativity of the constituents. The strength of metal–metal bonding is related to the cohesive energy which can be measured by heats of atomization shown in Fig. 4 for the three transition metal series. In the present case, gold, with much higher cohesive energy (368 kJ mol^{-1} for Au vs. 285 kJ mol^{-1} for Ag), tends to prefer interstitial sites such as the centers of icosahedra (rule 1) or the shared vertices (rule 2). As far as the metal–ligand bonding is concerned, the more electron-donating phosphine ligands prefer to coordinate to the more electronegative Au atoms (rule 3), whereas the more electron-withdrawing halide ligands prefer to interact with the more electropositive Ag atoms (rule 6). In terms of electronegativity, which is related to relativistic effects [17], the more electronegative gold atoms (2.54 for Au vs. 1.93 for Ag) prefer sites of high electron densities (such as the centers of icosahedra or the shared vertices) whereas the more electropositive silver atoms tend to occupy either surface sites (at the boundary of adjacent icosahedra) bridged by halide ligands (rule 4) or capping positions with high halide coordination (rule 5).

3.1.2. Trimetallic Au–Ag–M (M = group 10 metals) supraclusters

For mixed group 10 (M)–group 11 polyicosahedral clusters such as the trimetallic Au–Ag–M supraclusters (M = Pt, Pd, Ni) [25,26], the site preference (again referring to Table 1) can be attributed to the relative strengths of metal–metal and metal–ligand interactions as well as disparities in electronegativity: (1) group 10 metals prefer interstitial sites such as the centroids of icosahedra owing to their high cohesive energies (M > Au > Ag) that lead to stronger metal–metal bonds (see Fig. 4) [25]; (2) among the group 11 metals, Au prefers the interstitial sites such as the centers of icosahedra or the shared vertices owing to its high cohesive energy and high

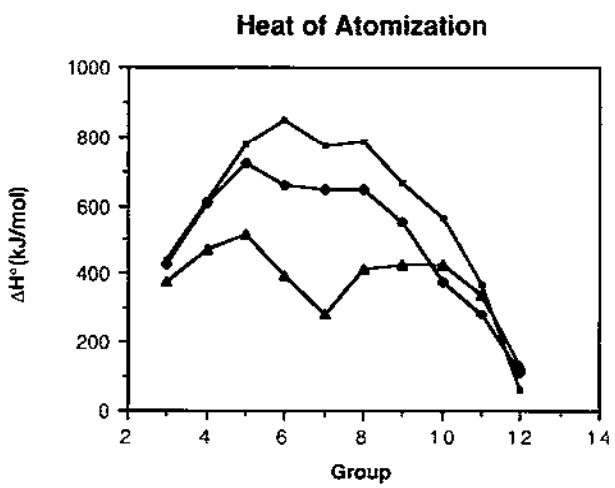

Fig. 4. Enthalpies of atomization (M(s)→M(g)) of the first (▲), second (◆), and third (■) transition metal series.

electronegativity (Au > Ag); (3) as far as the metal–ligand bonding is concerned, the more electronegative Au prefers phosphine coordination while the more electropositive Ag prefers halide coordination or halide bridging.

The structures of the trimetallic biicosahedral clusters $[(Ph_3P)_{10}Au_{12}Ag_{12}MCl_7]^+$ (M = Pt, Ni) [25,26] are portrayed in Fig. 5 and Fig. 6 respectively. Here, the metal core of an individual cluster can be described as two Au_6Ag_6 icosahedra, one M centered (M = Pt, Ni) and one Au centered, sharing a common Au atom. The arrangement of the four metal pentagons has an exact ses (staggered–eclipsed–staggered) configuration. The Au—Ag—Ni cluster [25b] is the first example of a polyicosahedral structure containing first, second, and third row transition metals; as such it opens the door to other trimetallic polyicosahedral clusters containing Au, Ag, and Ni. The Au—Ag—Ni cluster [25b] also represents the first example in which a first row transition metal is incorporated into a polyicosahedral cluster.

We have also synthesized the series $[(Ph_3P)_{10}Au_{11}Ag_{12}M_2Cl_7]$ where M = Pt, Pd, Ni [26] via the "preformed clusters" strategy. Other biicosahedral target molecules are depicted in Table 2. We should add that a related cluster $[(Ph_3P)_{10}Au_{11}Ag_{12}Pt_2Cl_7]$ has also been synthesized and structured by Steggerda and coworkers [31]. The shared vertex in this latter cluster, however, is Ag rather than Au.

We plan to extend our work to trimetallic triicosahedral supraclusters via the same synthetic strategy. For example, as depicted in Fig. 7, incorporation of one, two, and three group 10 metals into the biicosahedral cluster $[L_{12}Au_{18}Ag_{18}X_8]^{4+}$ produces $[L_{12}Au_{17}Ag_{18}MX_8]^{3+}$, $[L_{12}Au_{16}Ag_{18}M_2X_8]^{2+}$, and $[L_{12}Au_{15}Ag_{18}M_3X_8]^+$ respectively. Similar consideration applies to the other members (tetraicosahedral, pentaicosahedral etc.) of the series.

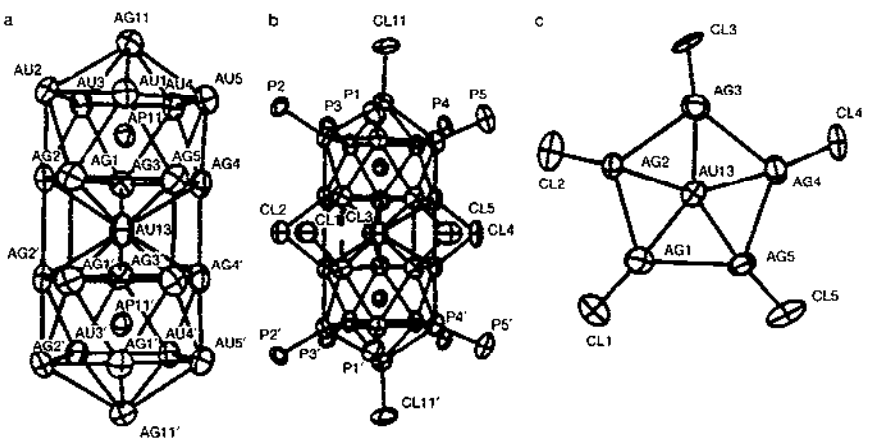

Fig. 5. Molecular architecture of $[(Ph_3P)_{10}Au_{12}Ag_{12}PtCl_7]^+$, as the Cl^- salt: (a) the metal core, $Au_{12}Ag_{12}Pt$; (b) the metal–ligand framework, $P_{10}Au_{12}Ag_{12}PtCl_7$; (c) projection of the two silver pentagons onto the five doubly bridging chloride ligands Cl1–Cl5. Atoms AP11 and AP11′ (centers of icosahedra) represent an equal admixture of Au and Pt owing to the crystallographically imposed mirror (*Cs-m*) symmetry.

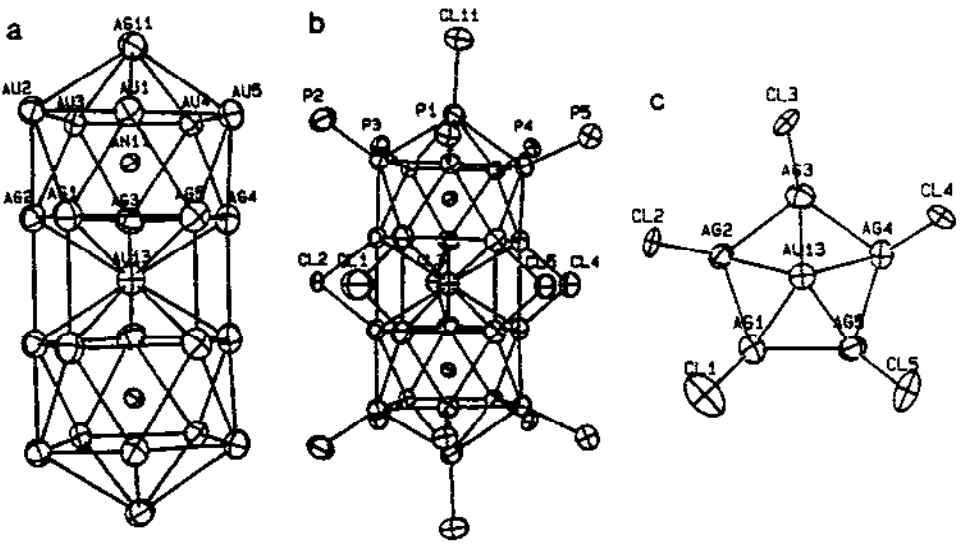

Fig. 6. Molecular architecture of $[(Ph_3P)_{10}Au_{12}Ag_{12}NiCl_7]^+$, as the SbF_6^- salt: (a) the metal core, $Au_{12}Ag_{12}Ni$; (b) the metal–ligand framework, $P_{10}Au_{12}Ag_{12}NiCl_7$; (c) projection of the two silver pentagons onto the five doubly bridging chloride ligands Cl1–Cl5. Atoms AN11 and AN11′ (centers of icosahedra) represent an equal admixture of Au and Ni owing to the crystallographically imposed mirror (*Cs-m*) symmetry.

Extended Hückel molecular orbital (EHMO) calculations have been performed on the bimetallic cluster $[(R_3P)_{10}Au_{13}Ag_{12}Cl_7]^{2-}$, where R = H, in order to assess the electronic origins of the site preference principles. These site preference principles, and their bonding implications, are rationalized via simple bond strength vs. charge accumulation (BSCA) plots [25b].

3.2. Metal–ligand interactions: bulk-to-surface and surface-to-surface segregations

It is well known that the surface of bimetallic particles often has a different composition to its interior. Thermodynamic causes for this "surface enrichment" have been discussed in the literature [29]. There are also kinetic factors which favor certain arrangements of metal atoms in mixed clusters. Metal–ligand interactions play an important role in dictating the surface composition of a multimetallic cluster. Here we may distinguish between two kinds of surface enrichment and/or segregation processes. The first type is analogous to the so-called "chemisorption-induced surface segregation" [34] whereby strong metal–ligand interactions cause a surface enrichment of metal atoms which would otherwise prefer interstitial (bulk) sites. For example, Au—Pt alloy particles should have a Pt-rich core (kernel) and a Au-rich surface (mantle) owing to the high cohesive energy of Pt vs. Au. This is the so-called "cherry" model. Exposure to a CO atmosphere, however, causes an enrichment of platinum atoms at the surface as a result of the strong and selective interactions

Table 2
Examples of bimetallic (AuAg) and trimetallic (AuAgM where M = Pt, Pd, Ni) biicosahedral clusters in the 6-ring (left) and 5-ring (right) series

$[L_{10}M_{25}X_8]^{q+}$	$[L_{10}M_{25}X_7]^{q+}$
SATELLITE RING MODEL[a]	
6-ring	5-ring
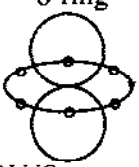	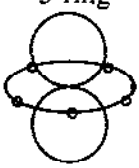
BIMETALLIC	
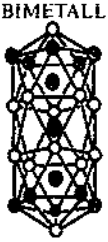 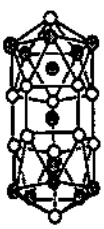	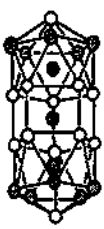
sss sss	ses
$[(Ph_3P)_{10}Au_{13}Ag_{12}Br_8]^+$	$[(p\text{-}tol_3P)_{10}Au_{13}Ag_{12}Cl_7]^{2+}$
TRIMETALLIC	
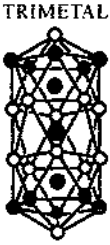 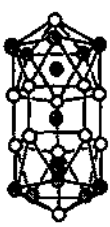	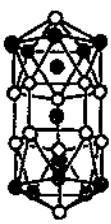
sss ses	scs
	1, 4
$[(R_3P)_{10}Au_{12}Ag_{12}MX_8]$	$[(Ph_3P)_{10}Au_{12}Ag_{12}MCl_7]^+$
REMARKS Au/Ag/M= ●/○/● M=Pt, Pd, Ni	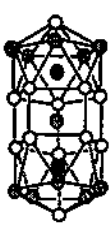
	ses
	$[(R_3P)_{10}Au_{11}Ag_{12}M_2X_7]$

Only ses (R(0)) and sss (R(36)) rotamers are shown though other intermediate metal configurations (R(Θ)) are also possible (see Fig. 13). Note that each substitution of an interstitial Au atom by a group 10 metal decreases the overall charge by 1.

[a]satellite ring (ellipse) of bridging ligands (⊃) around two metal icosahedra (○).

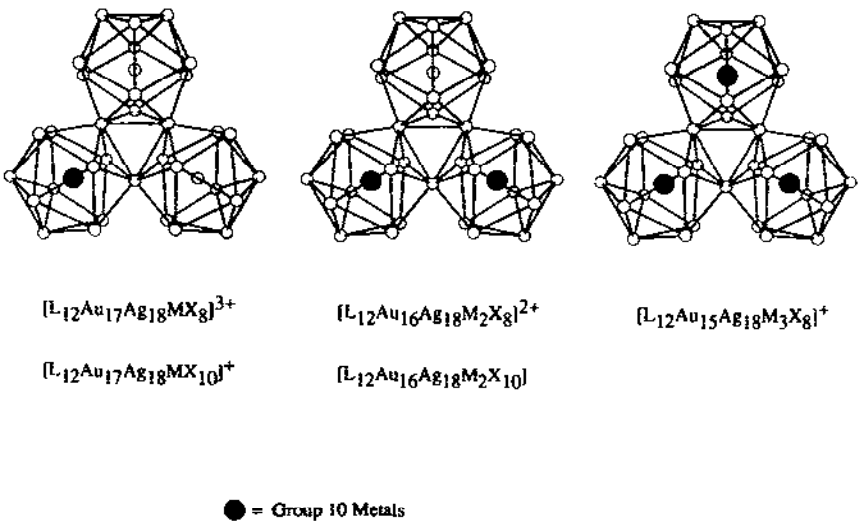

Fig. 7. *endo* icosahedral chemistry: trimetallic (Au−Ag−M) triicosahedral clusters with one, two, and three group 10 (M = Pt, Pd, Ni) metals at the center(s) of icosahedra.

between CO and Pt atoms. This results in a Au-rich core and a Pt-rich surface [34a], thereby causing an "inversion" of the "cherry" model.

The second type of "surface segregation" is exemplified by the series of bi- and trimetallic polyicosahedral clusters characterized by us [11,22–26]. As discussed in the previous section, the more electronegative surface Au atoms prefer the more electron-donating phosphines as ligands whereas the less electronegative surface Ag atoms prefer coordination with the more electronegative halide ligands. In other words, preferential metal–ligand bindings may cause segregation of Au and Ag atoms on the surface of a cluster.

In short, strong, selective metal–ligand bonding can cause either a "bulk-to-surface" inversion (first type) or a "surface-to-surface" segregation (second type).

4. Stereochemical principles

4.1. Rotamerism: the biicosahedral rotor model

Structural studies of the cluster $[(Ph_3P)_{10}Au_{13}Ag_{12}Br_8]^+$ in two crystal forms containing different anions revealed two distinct conformers with different metal configurations (Fig. 8), the staggered–eclipsed–staggered (ses) in the SbF_6^- salt [11c] and the staggered–staggered–staggered (sss) configuration in the Br^- salt [11e] as portrayed in Figs. 9 and 10 respectively. This new type of cluster isomerism has been coined "rotamerism". The observation of both rotamers (ses and sss) for the same cluster led to the recognition that this biicosahedral cluster series may serve as a

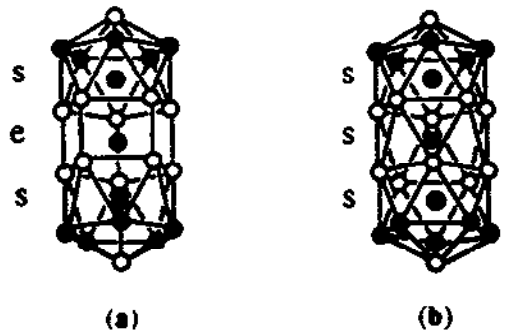

Fig. 8. Two extreme rotameric forms of the vertex-sharing biicosahedral supraclusters: (a) staggered–eclipsed-staggered (ses) and (b) staggered–staggered–staggered (sss).

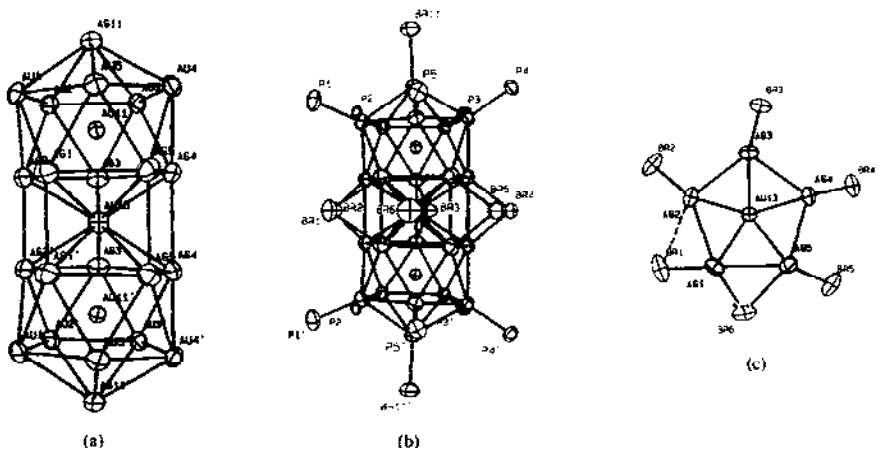

Fig. 9. Molecular architecture of $[(Ph_3P)_{10}Au_{13}Ag_{12}Br_8](SbF_6)$: (a) the ses metal core; (b) metal–ligand framework; (c) projection of the two Ag_5 pentagons and six Br ligands as viewed along idealized fivefold axis.

prototype for molecular mechanical rotary devices, with possible utilities in nanotechnology [28].

More examples of rotamerism are needed in order to determine the cause and effect of this new type of cluster isomerization. This can be done by employing different anions or solvents. Knowing the cause and effect of rotamerism will allow us to control its stereochemistry and properties. Such controls are essential in device fabrication and engineering.

Fig. 11 shows the structure of $[(p\text{-}tol_3P)_{10}Au_{13}Ag_{12}Cl_8]^+$ [11d]. Distinct from previously observed structures, the adjacent metal pentagons in this cluster adopt neither sss nor ses configuration. In fact, it is nearly halfway between these two

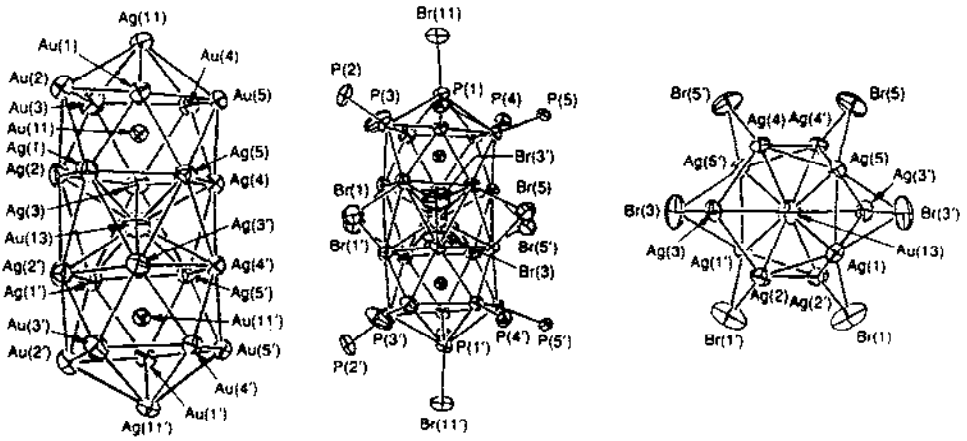

Fig. 10. Molecular architecture of $[(Ph_3P)_{10}Au_{13}Ag_{12}Br_8](Br)$: (a) the sss metal core; (b) metal–ligand framework; (c) projection of two Ag_5 pentagons and six Br ligands as viewed along idealized fivefold axis.

extremes (cf. Fig. 11(c)). This new metal configuration strongly suggests that the observed solid state structure represents a "snapshot" of a "molecular rotor" in motion.

It occurs to us that the metal core of this class of 25-metal-atom supraclusters may conceptually be described as a molecular biicosahedral rotor. The relative rotation of the two icosahedra about the shared vertex gives rise to various metal configurations called "rotamers" [11e]. This "biicosahedral rotor" model may be represented by the caricature depicted in Fig. 12(a).

An important question that needs to be addressed is whether or not this mode of rotation is quantized. In other words, are there magic numbers (such as $9n$), shown in Fig. 13, which Θ must conform to? If it is not quantized, then the two metal icosahedra are relatively "free" to rotate (fluxional) about the shared vertex (at least in solution), and the observed solid state structure merely represents a "snapshot" of one of many local (shallow) energy minima. We plan to synthesize biicosahedral rotamers, $R(\Theta)$, of different Θ values with the hope of resolving this issue.

4.2. *Roulettamerism: the satellite ring model*

Two series of biicosahedral metal clusters of the general formulae $[(R_3P)_{10}Au_{13}Ag_{12}X_7]^{2+}$ (the 5-ring series) and $[(R_3P)_{10}Au_{13}Ag_{12}X_8]^{+}$ (the 6-ring series) have been synthesized and structured by us [11]. A detailed analysis of the structures revealed a stellated ring of five or six halide ligands bridging the two inner silver pentagons. In order to understand the interrelations among the various bridging ligand arrangements as well as the underlying stereochemical principles, we

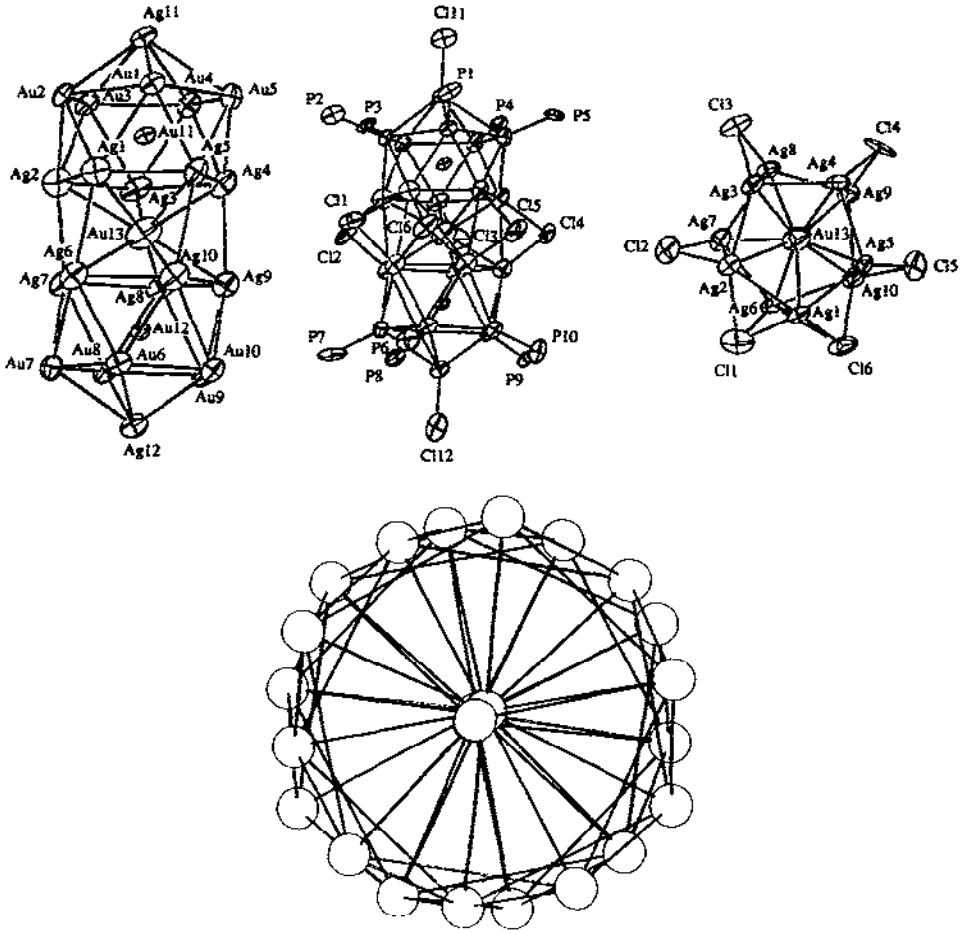

Fig. 11. A nanoscale molecular rotor: structure of $[(p\text{-tol}_3P)_{10}Au_{13}Ag_{12}Cl_8](PF_6)$ (a) metal core; (b) metal–ligand framework; (c) projection of two Ag_5 pentagons and six Br ligands; (d) projection of four metal pentagons along idealized fivefold axis.

propose a "satellite ring" model (Fig. 12(b)) [11f]. According to this model, five or six bridging ligands form a "satellite ring" around the "equator" of a particular rotameric biicosahedral metal core, resulting in the various bridging arrangements which have been coined "roulettamerism". The 5-ring and 6-ring "satellite" models are depicted schematically in Fig. 14(a) [11f]. Some known examples (except 3) of the bridging halide ligand arrangements are depicted in Fig. 14(b); qd_5 (1), *ortho*-$qq'd_4$ (2), *ortho*-q_2d_4 (3) of the R(0) or ses rotameric form, *ortho*-t_2d_4 (4) of the R(18) rotamer, *para*-d_2t_4 (5) and *para*-t_2d_4 (6) of the R(36) or sss rotamer in the 6-ring series. The chemical formulae of these examples are tabulated in Table 3. Here only the two inner silver pentagons and the bridging halide ligands are shown. Note also that d, t, and q designate doubly, triply, and quadruply bridging respectively.

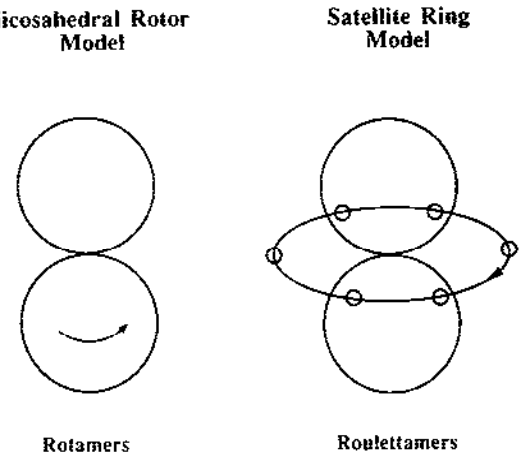

Fig. 12. (a) Biicosahedral rotor model gives rise to various rotamers of the metal core. (b) Satellite ring model of the various bridging arrangements gives rise to different roulettamers.

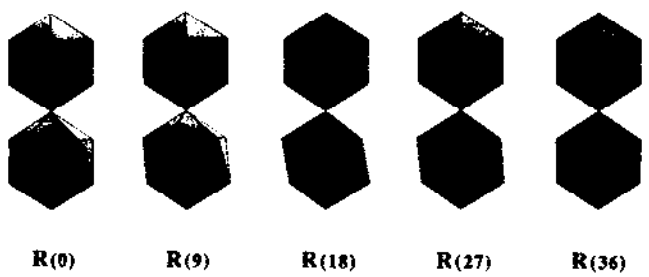

Fig. 13. Molecular rotor: vertex-sharing biicosahedral rotors R(Θ) with relative rotations $\Theta = 0$ (ses), 9°, 18°, 27° and 36° (sss) between the two icosahedra.

The 5-ring series is portrayed in Fig. 14(c). Here only the d_5 roulettameric form of the R(0) or ses metal configuration has been observed so far.

Work is in progress to find new bridging ligand environments (i.e. roulettamers).

4.3. Cluster cavity chemistry: the "Venus flytrap" analogy

The stereochemistry of clusters $[(Ph_3P)_{14}Au_{18}Ag_{20}Cl_{12}]^{2+}$ (**1**) [11k], $[(p\text{-}tol_3P)_{12}Au_{18}Ag_{20}Cl_{14}]$ (**2**) [11h], and $[(Ph_3P)_{12}Au_{18}Ag_{19}Cl_{11}]^{2+}$ (**3**) [11m] led to the concept of "intracavity" chemistry on the "surface" of a metal cluster [11k]. Fig. 15 depicts schematically the size and shape of the cavities in **1** and **2** (after removal of the $[Ph_3PAgCl_3]$ and $[AgCl_4]$ moieties respectively). It can be seen that the accessible "metal surface" of these clusters is the Ag_3 triangle, "picket fenced" by three aryl groups (shaded) from three separate phosphine ligands. Also shown is the cavity on the μ_3-Cl side of **3** which is completely sealed off by three phenyl rings (shaded). The ability of the cavities in **1–3** to expand and contract is to a large

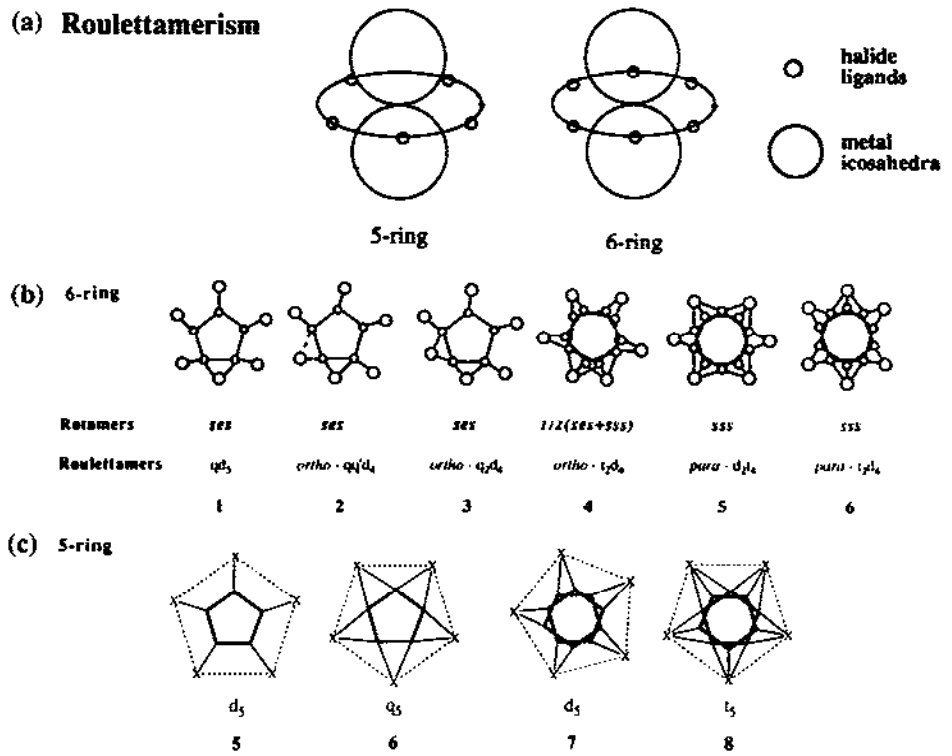

Fig. 14. (a) Two series of biicosahedral metal clusters of general formulae $[(R_3P)_{10}Au_{13}Ag_{12}X_7]^{2+}$ (the 5-ring series) and $[(R_3P)_{10}Au_{13}Ag_{12}X_8]^{+}$ (the 6-ring series), giving rise to various bridging ligand arrangements (roulettamers). (b) Projections of the two inner silver pentagons onto the equatorial plane of the six halide ligands for some representative vertex-sharing biicosahedral supraclusters showing the various metal configurations (rotamers) and ligand arrangements (roulettamers) for the 6-ring series (see Table 3 for examples). (c) Same as (b) for the 5-ring series.

Table 3
Examples of the 6-ring biicosahedral series

1	$[(Ph_3P)_{10}Au_{13}Ag_{12}Cl_8](SbF_6)$	[11f]
2	$[(Ph_3P)_{10}Au_{13}Ag_{12}Br_8](SbF_6)$	[11c]
4	$[(p\text{-}tol_3P)_{10}Au_{13}Ag_{12}Cl_8](PF_6)$	[11d]
5	$[(p\text{-}tol_3P)_{10}Au_{13}Ag_{12}Br_8](PF_6)$	[11b]
6	$[(Ph_3P)_{10}Au_{13}Ag_{12}Br_8](Br)$	[11e]

extent due to the fact that the shared vertices resemble flexible connectors which allow individual icosahedral units to twist around, thereby causing conformational changes of the phosphine ligands. The existence of the accessible, "picket-fenced" metal surfaces as well as the flexible (structurally non-rigid) cavities on the surface of a large metal cluster, both of which can easily be tailored to incoporate a variety of guest molecules, may have further implications in the studies of inclusion com-

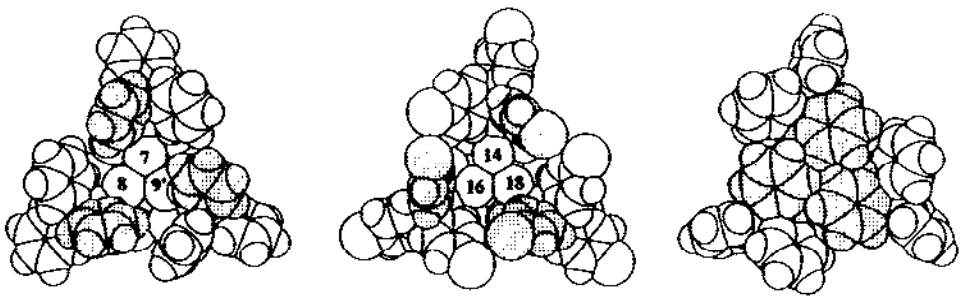

Fig. 15. Cluster cavity chemistry and the Venus flytrap analogy: space-filling models for cluster surface cavities of $[(Ph_3P)_{14}Au_{18}Ag_{20}Cl_{12}]^{2+}$ (1), $[(p\text{-}tol_3P)_{12}Au_{18}Ag_{20}Cl_{14}]$ (2), and $[(Ph_3P)_{12}Au_{18}Ag_{19}Cl_{11}]^{2+}$.

plexes, metal surfaces, and catalysis. It occurs to us that this "breeding" mode will allow the cluster to capture a variety of small molecules or ions in a way similar to the Venus flytrap (Fig. 16). The interactions (and the driving force) may range from

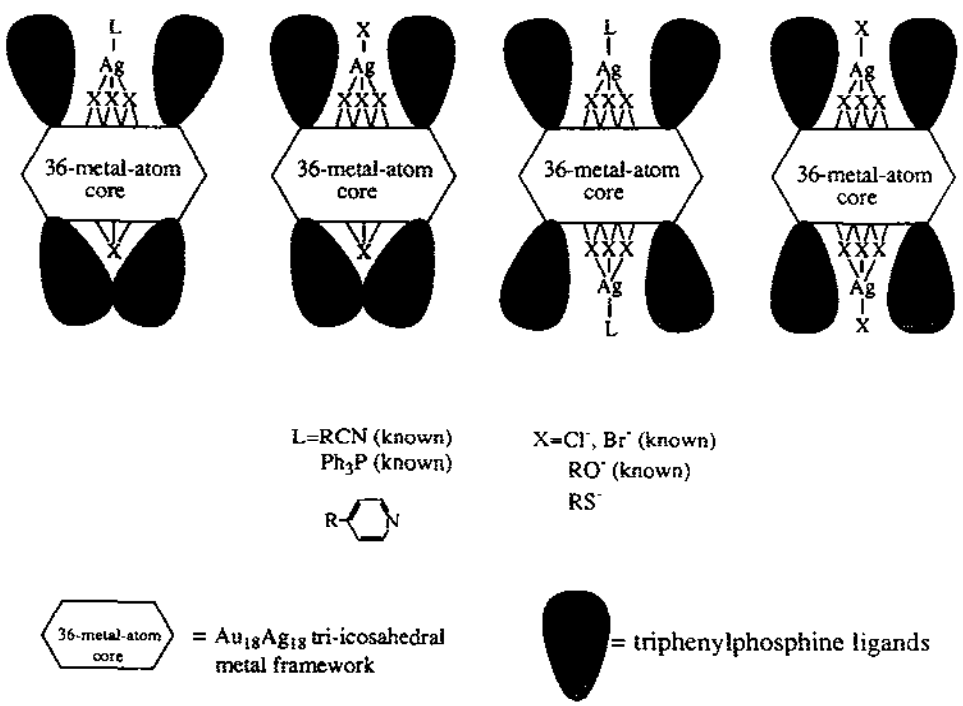

Fig. 16. The "Venus flytrap" analogy of the cluster cavity chemistry of the 37 (left) and 38 (right) triicosahedral clusters.

strong covalent or ionic bonding to weak van der Waals or hydrogen bonding. In addition to $[Ph_3PAgX_3]$ (as in **1**), $[AgX_4]$ (as in **2**), or μ_3-X (as in **3**) moieties (X = halides), our preliminary results show that other functional groups or solvent molecules can also be incorporated into the cavities (via coordination to the capping Ag atoms) [32], as indicated in Fig. 16.

A detailed examination of the surface of biicosahedral cluster $[(Ph_3P)_{10}Au_{13}Ag_{12}Br_8]^-$ also revealed that there are "corridors" along the idealized fivefold axis of the cluster as well as "cracks" in the equatorial plane as shown in Fig. 17 [32b]. These are the localities where the terminal and bridging halide ligands are situated (or buried). As such, the crystal structure is more or less independent of the size (Cl vs. Br), or the number (five or six), of the bridging halide ligands.

5. Conclusions and future prospects

In conclusion, this review highlights our work on large mixed-metal clusters which has given rise to a series of bi- and trimetallic vertex-sharing polyicosahedral clusters [11,22–26]. The synthetic strategies and structural systematics of this new class of clusters allow us to formulate the concept of "cluster of clusters". The most important characteristics of this series of clusters of clusters are its precise design rules and growth sequence. These characteristics are highly desirable in that they allow us to develop (1) *endo* icosahedral chemistry by incorporating group 10 metals in the centers of the icosahedra, (2) *exo* icosahedral chemistry by capping the icosahedral faces or by "capturing" small molecules in the cluster cavities, and (3) framework icosahedral chemistry by changing the metal combination (group 11 metals) of the cluster architecture. New directions include, but are not limited to, (1) new synthetic strategy based on "performance clusters", (2) incorporation of group 10 metals (Pt,Pd,Ni) in the icosahedral holes, (3) new concepts such as rotamerism and rouletamerism, and (4) new intracavity chemistry resembling Venus flytrap.

The successful synthesis of trimetallic polyicosahedral clusters [25,26] discussed in this review suggest the existence of a parallel sequence of trimetallic (Au—Ag—M

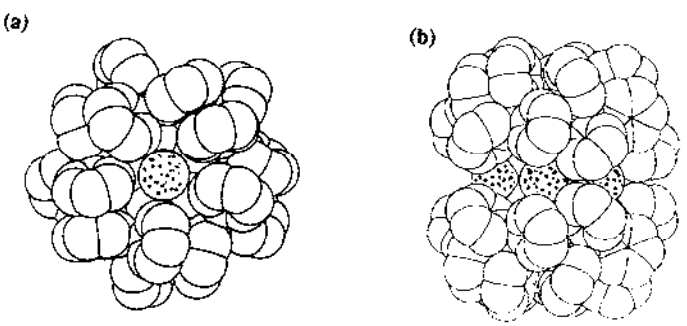

Fig. 17. The cluster cavities of $[(Ph_3P)_{10}Au_{13}Ag_{12}Br_8]^+$ in the $qq'd_4$-ses configuration: (a) "corridors" along the idealized fivefold axis; (b) "cracks" in the equatorial plane.

where M is a transition metal) vertex-sharing polyicosahedral supraclusters, from a single icosahedron of 13 metal atoms to an icosahedron of icosahedra of 127 metal atoms, in analogy to the bimetallic (Au—Ag) vertex-sharing polyicosahedral clusters [11,22,23]. Here the vertex-sharing polyicosahedral cluster architecture (framework chemistry) is provided by the coinage metals (Au and Ag or Au and Cu) while the icosahedral holes (*endo* chemistry) or the capping sites (*exo* chemistry) are occupied by a third metal M. It is also possible to generalize this scheme to tetra- and pentametallic polyicosahedral sequence. Indeed we have begun to investigate tetra- and pentametallic biicosahedral clusters such as $[L_{10}Au_{11}Ag_{12}PtNiX_7]$ and pentametallic triicosahedral clusters such as $[L_{12}Au_{15}Ag_{18}PtPdNiX_8]^+$ depicted in Figs. 18(a) and 18(b) respectively. In these examples, the stereochemical principles in general and site preference in particular developed so far allow us to predict that group 10 metals will occupy the centers of the Au—Ag polyicosahedral framework.

The multimetallic polyicosahedral cluster series allows us to study the site preference and alloy formation of multimetallic systems or phases in a well-defined way. The site preference rule can be rationalized in terms of the disparities in metal–metal vs. metal–ligand bonding strengths. As far as metal–metal bonding is concerned, the site preference rules can be understood with the aid of BSCA plots [25b]. Here the metal–metal bonding strengths are estimated from the cohesive energy whereas the charge accumulation powers are based on Pauling's electronegativity. The importance of metal–ligand bonding in dictating surface segregation and/or enrichments has also been discussed [25b]. These qualitative bonding pictures are supported by

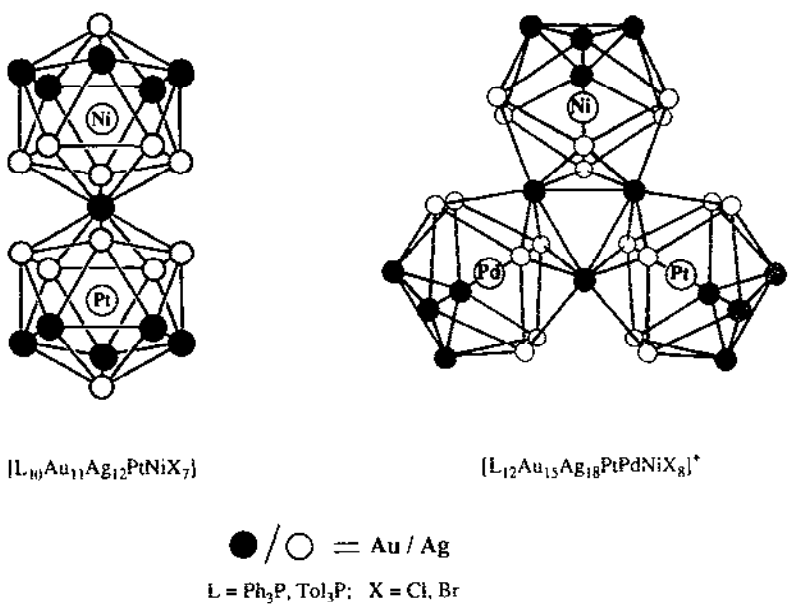

Fig. 18. (a) An example of tetrametallic (AuAgPtNi) vertex-sharing biicosahedral clusters. (b) An example of pentametallic (AuAgPtPdNi) vertex-sharing triicosahedral clusters.

EHMO calculations. Electron counting rules (such as the Polyoctet rule [22b,23e] and Cluster of Cluster (C^2) model [23e,23f]), as applied to multimetallic icosahedral and polyicosahedral clusters , have also been developed by us [22–24]. It is hoped that basic understanding of the stereochemical and bonding principles governing alloy formation in multimetallic clusters will lead to better electronic and stereochemical controls of their structures and reactivities and, ultimately, to better design and manufacture or fabrication of structurally well-defined and functionally optimized nanoarchitecture [28], multimetallic catalysts [29] etc.

We should emphasize that the same synthetic strategies and methodologies described in this review can be applied to other multimetallic polyicosahedral supraclusters as well. For example, recently we have extended our study to other polyicosahedral supraclusters involving early transition metals such as group 5 (V,Nb,Ta), group 6 (Cr,Mo,W) and group 7 (Mn,Re). These early transition metals are chosen based on the consideration of their high cohesive energies (Fig. 4) and hence their capabilities to form strong metal–metal bonds. In accordance with the site preference principles established so far, we predict that group 5–7 metals, with their high cohesive energies, will occupy the centers of the icosahedra, thereby strengthening the structure of the cluster, as illustrated in Fig. 19.

The structural and bonding principles developed here for vertex-sharing polyicosahedral clusters may also be applicable to other multimetallic systems or phases,

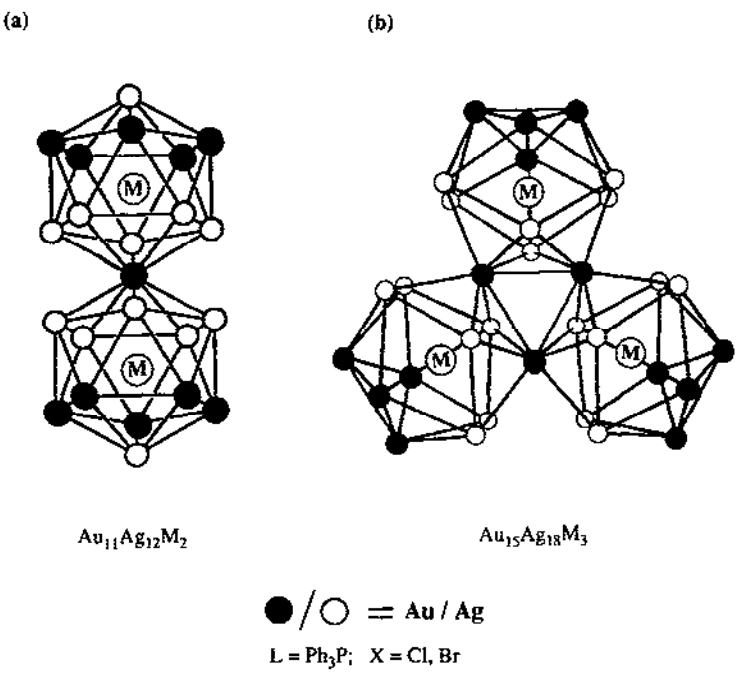

Fig. 19. Examples of (a) biicosahedral and (b) triicosahedral trimetallic clusters Au—Ag—M where M = group 5 (V,Nb,Ta), 6 (Cr,Mo,W), and 7 (Mn,Re).

even though the geometry and symmetry may be different for different systems and the terminology may be different in different technologies. For example, terms such as site preference, interstitial vs. surface sites in metal cluster chemistry are equivalent to terms such as segregation (surface enrichment), interior (kernel) vs. exterior (mantle) often used in catalysis or metallurgy.

Finally, it is apparent that the icosahedral geometry and symmetry play an important role in the structure and bonding, as well as the nucleation and growth, of many cluster systems (especially for, but by no means limited to, "electron-deficient" clusters). Furthermore, it occurs to us that the vertex-sharing polyicosahedral sequence could be a fairly common growth pathway for a wide variety of multimetallic particles in the nanorealm. The tendency for such growth behaviour may be coined "polyicosahedricity".

Acknowledgment

Acknowledgment is made to the National Science Foundation (CHE-9115278) for financial support of this research.

References

[1] F.A. Cotton, Chemical Applications of Group Theory, Wiley, New York, 2nd edn., 1971.
[2] (a) R. N. Grimes, Carboranes, Academic Press, New York, 1970.
(b) H. Beall, in E.L. Muetterties (ed.), Boron Hydride Chemistry, Academic Press, New York, 1975, p. 301.
[3] (a) W.N. Lipscomb and J.A. Wunderlich, J. Am. Chem. Soc., 82 (1960) 4427.
(b) E.L. Muetterties, R.E. Merrifield, H.C. Miller, W.H. Knoth and J.R. Downing, J. Am. Chem. Soc., 84 (1962) 2506.
[4] (a) V.G. Albano, F. Demartin, M.C. Iapalucci, F. Laschi, G. Longoni, A. Sironi and P. Zanello, J. Chem. Soc., Dalton Trans., (1991) 739.
(b) V.G. Albano, F. Demartin, M.C. Iapalucci, G. Longoni, A. Sironi and V. Zanotti, J. Chem. Soc., Chem. Commun., (1990) 547.
(c) V.G. Albano, F. Demartin, M.C. Iapalucci, G. Longoni, M. Monan and P. Zanello, J. Chem. Soc., Dalton Trans., (1992), 497.
(d) V.G. Albano, F. Demartin, M.C. Iapalucci, G. Longoni, M. Monan, P. Zanello and A. Sironi, J. Chem. Soc., Dalton Trans., (1993) 173.
[5] (a) D.F. Rieck, J.A. Gavney Jr., R.L. Norman, R.K. Hayashi and L.F. Dahl, J. Am. Chem. Soc., 114 (1992) 10369.
(b) D.F. Rieck, R.A. Montag, T.S. McKechnie and L.F. Dahl, J. Am. Chem. Soc., 108 (1986) 1330.
(c) R.E. DesEnfants II, J.A. Gavney Jr., R.K. Hayashi and L.F. Dahl, J. Organomet. Chem., 383 (1990) 543.
(d) J.P. Zebrowski, R.K. Hayashi and L.F. Dahl, J. Am. Chem. Soc., 115 (1993) 1142.
[6] A.J. Kahaian, J.B. Thoden and L.F. Dahl, J. Chem. Soc., Chem. Commun., (1992) 353.
[7] A. Ceriotti, F. Demartin, B.T. Heaton, P. Ingallina, G. Longoni, N. Manassero, M. Marchionna and N. Masciocchi, J. Chem. Soc., Chem. Commun., (1989) 786.
[8] J.L. Vidal and J.M. Troup, J. Organomet. Chem., 213 (1981) 351.

[9] (a) C.E. Briant, B.R.C. Theobald, J.W. White, L.K. Bell and D.M.P. Mingos, J. Chem. Soc., Chem. Commun., (1981) 201.
(b) C.E. Briant, K.V. Hall and D.M.P. Mingos, J. Chem. Soc., Chem. Commun., (1984) 290.
[10] W.H. Knoth, Inorg. Chem., 10 (1971) 598.
[11] (a) B.K. Teo and K. Keating, J. Am. Chem. Soc., 106 (1984) 2224.
(b) B.K. Teo, H. Zhang and X. Shi, Inorg. Chem., 29 (1990) 2083.
(c) B.K. Teo, X. Shi and H. Zhang, J. Am. Chem. Soc., 113 (1991) 4329.
(d) B.K. Teo and H. Zhang, Angew. Chem., Int. Edn. Engl., 31 (1992) 445.
(e) B.K. Teo, X. Shi and H. Zhang, J. Chem. Soc., Chem. Commun., (1992) 1195.
(f) B.K. Teo, X. Shi and H. Zhang, J. Cluster Sci., 4(4) (1993) 471.
(g) B.K. Teo and H. Zhang, Inorg. Chem., 30 (1991) 3115
(h) B.K. Teo, H. Zhang and X. Shi, J. Am. Chem. Soc., 112 (1990) 8552.
(i) B.K. Teo, M. Hong, H. Zhang, D. Huang and X. Shi, J. Chem. Soc., Chem. Commun., (1988) 204.
(j) B.K. Teo, M. Hong, H. Zhang and D. Huang, Angew. Chem., Int. Edn. Engl., 26 (1987) 897.
(k) B.K. Teo, X. Shi and H. Zhang, Inorg. Chem., 32 (1993) 3987.
(l) B.K. Teo, X. Shi and H. Zhang, cited in Chem. Eng. News, 67 (1989) 6.
(m) B.K. Teo, X. Shi and H. Zhang, unpublished work.
[12] J.L. Hoard and R.E. Hughes, in E.L. Muetterties (ed.), The Chemistry of Boron and Its Compounds, Wiley, New York, 1967, p. 25.
[13] D. Emin, T. Aselage, C.L. Beckel, I.A. Howard and C. Wood (eds.), Boron-Rich Solids, American Institute of Physics Conference Proceedings 140, American Institute of Physics, New York, 1986.
[14] (a) C. Belin, Acta Crystallogr. B, 37 (1981) 2060.
(b) C. Belin, Acta Crystallogr. B, 36 (1980) 1339.
[15] (a) D. Levine and P.J. Steinhardt, Phys. Rev. Lett., 53 (1984) 2477.
(b) D. Levine and P.J. Steinhardt, Phys. Rev. B, 34 (1986) 596.
[16] B.K. Teo, X. Shi and H. Zhang, J. Am. Chem. Soc., 114 (1992) 2743.
[17] (a) A. Grohmann, J. Riede and H. Schmidbaur, Nature (London), 345 (1990) 140.
(b) F. Scherbaum, A. Grohmann, G. Muller and H. Schmidbaur, Angew. Chem., Int. Edn. Engl., 28 (1989) 463.
(c) H. Schmidbaur, W. Graf and G. Muller, Angew. Chem., Int. Edn. Engl., 27 (1988) 417.
(d) H. Schmidbaur, F. Scherbaum, B. Huber and G. Muller, Angew. Chem., Int. Edn. Engl., 27 (1988) 419.
(e) P. Pyykko and J. Desclaux, Acc. Chem. Res., 12 (1979) 276.
(f) K.S. Pitzer, Acc. Chem. Res., 12 (1979) 271.
[18] (a) D.F. Shriver, H.D. Kaesz and R.D. Adams (eds.), The Chemistry of Metal Cluster Complexes, VCH, New York, 1990.
(b) B.F.G. Johnson (ed.), Transition Metal Clusters, Wiley Interscience, Chichester, 1980.
[19] (a) C.M.T. Hayward, J.R. Shapley, M.R. Churchill, C. Bueno and A.L. Rheingold, J. Am. Chem. Soc., 104 (1982) 7347.
(b) E.G. Mednikov, N.K. Eremenko, Yu.L. Slovokhotov and Yu.T. Struchkov, J. Chem. Soc., Chem. Commun., (1987) 218.
(c) E.G. Mednikov and N.K. Eremenko, J. Organomet. Chem., C35–C37 (1986) 301.
(d) D. Fenske and H. Krautscheid, Angew. Chem., Int. Edn. Engl., 29 (1990) 1452.
(e) M.W. Payne, D.L. Leussing and S.G. Shore, J. Am. Chem. Soc., 109 (1987) 617.
(f) M.M. Amini, T.P. Fehlner, G.J. Long and M. Politowski, Chem. Mater., 2 (1990) 432.
(g) J.S. Bradley, in M. Moskovits (ed.), Metal Clusters, Wiley, New York, 1986, Chap. 5, p. 105.
(h) R.D. Willett, J. Coord. Chem., 19 (1988) 253.
(i) T.W. Koenig, B.P. Hay and R.G. Finke, Polyhedron, 7 (1988) 1479.
(j) K.H. Whitmire, J. Coord. Chem., 17 (1988) 95.
(k) M. Ichikawa, Chem. Technol., (1982) 674.
(l) J.W. Lauher, J. Organomet. Chem., 213 (1981) 25.
(m) A.J. Whoolery and L.F. Dahl, J. Am. Chem. Soc., 113 (1991) 6683.

(n) R.W. Broach, L.F. Dahl, G. Longoni, P. Chini, A.J. Schultz and J.M. Williams, Adv. Chem. Ser., 167 (1978) 93.
(o) G.P. Elliott, J.A.K. Howard, T. Mise, C.M. Nunn and F.G.A. Stone, Angew. Chem., Int. Edn. Engl., 25 (1986) 190.
(p) D.E. Smith, A.J. Welch, I. Treurnicht and R.J. Puddephatt, Inorg. Chem., 25 (1986) 4616.
[20] (a) P. Braunstein and J. Rose, in I. Bernal (ed.), Stereochemistry of Organometallic Inorganic Compounds, Vol. 3, Elsevier, Amsterdam, p. 320.
(b) W.L. Gladfelter and F.L. Geoffroy, Adv. Organomet. Chem., 18 (1980) 207.
(c) A.J. Amoroso, L.H. Gade, B.F.G. Johnson, J. Lewis, P.R. Raithby and W.-T. Wong, Angew. Chem., Int. Edn. Engl., 30 (1991) 107.
(d) M.H. Chisholm, ACS Symp. Ser., 155 (1981) 17.
(e) K.P. Callahan and M.F. Hawthorne, Adv. Organomet. Chem., 14 (1976) 145.
[21] (a) L.N. Ito, D.J. Sweet, A.M. Mueting, L.H. Pignolet, J.J. Steggerda and M.F.I. Schoondergang, Inorg. Chem., 28 (1989) 3696.
(b) R.P.F. Kanters, J.J. Bour, P.P.J. Schlebos, W.P. Bosman, H. Behm, J.J. Steggerda and L.H. Pignolet, Inorg. Chem., 28 (1989) 2591.
(c) J.J. Bour, R.P.F. Kanters, P.P.J. Schlebos and J.J. Steggerda, Recl. Trav. Chim. Pays-Bas, 107 (1988) 211.
(d) R.P.F. Kanters, P.P.J. Schlebos, J.J. Bour, W.P. Bosman, H. Behm and J.J. Steggerda, Inorg. Chem., 27 (1988) 4034.
(e) R.P.F. Kanters, P.P.J. Schlebos, J.J. Bour, W.P. Bosman, J.M.M. Smits, P.T. Buerskens and J.J. Steggerda, Inorg. Chem., 29 (1990) 324.
[22] (a) B.K. Teo and H. Zhang, Proc. Natl. Acad. Sci. USA, 88 (1991) 5067.
(b) B.K. Teo, H. Zhang and X. Shi, in A.J. Welch and S.K. Chapman (eds.), The Chemistry of the Copper and Zinc Triads, The Royal Society of Chemistry, London, 1993, pp. 211–234.
[23] (a) B.K. Teo and H. Zhang, J. Cluster Sci., 1 (1990) 223.
(b) B.K. Teo and H. Zhang, J. Cluster Sci., 1 (1990) 155.
(c) B.K. Teo and H. Zhang, Polyhedron, 9 (1990) 1985.
(d) B.K. Teo, Polyhedron, 7 (1988) 2317.
(e) B.K. Teo and H. Zhang, Inorg. Chem., 27 (1988) 414.
(f) B.K. Teo and H. Zhang, Inorg. Chem. Acta, 144 (1988) 173.
[24] B.K. Teo, H. Zhang, Y. Kean, H. Dang and X. Shi, J. Chem. Phys., 99 (1993) 2929.
[25] (a) B.K. Teo, H. Zhang and X. Shi, J. Am. Chem. Soc., 115 (1993) 8489.
(b) B.K. Teo, H. Zhang and X. Shi, Inorg. Chem., 33 (1994) 4086.
[26] B.K. Teo, H. Zhang and X. Shi, unpublished results, 1993.
[27] (a) B.B. Mandelbrot, The Fractal Geometry of Nature, Freeman, New York, 1983.
(b) H.O. Peitgen and P. Richter, The Beauty of Fractals, Springer, Heidelberg, 1986.
[28] (a) K.J. Klabunde, Chemistry of Free Atoms and Particles, Academic Press, New York, 1980.
(b) R.C. Baetzold, J. Chem. Phys., 55 (1971) 4363.
(c) G.D. Stucky, N. Herron, Y. Wang, M. Eddy, D. Cox, K. Moller and T. Bein, J. Am. Chem. Soc., 111 (1989) 530.
(d) G.D. Stucky, J.E. MacDougall, H. Eckert, N. Herron, Y. Wang, K. Moller and T. Bein, J. Am. Chem. Soc., 111 (1989) 8006.
(e) K. Moller, A. Borvornwattananont and T. Bein, J. Chem. Phys., 93 (1989) 4562.
(f) A. Borvornwattananont, K. Moller and T. Bein, J. Chem. Phys., 93 (1989) 4205.
[29] (a) W.M.H. Sachtler and R.A. van Santen, Adv. Catal., 26 (1977) 69.
(b) J.H. Sinfelt, Bimetallic Catalysts: Discoveries, Concepts, and Applications, Wiley, New York, 1983, pp. 1–164, and references cited therein.
(c) B.C. Gates, L. Guczi and H. Knozinger, Metal Clusters in Catalysts, Elsevier, Amsterdam, 1988.
(d) K.H. Whitmire, J. Coord. Chem., 17 (1988) 95.
(e) M. Boudart, Adv. Catal., 20 (1969) 153.
(f) M. Boudart, J. Mol. Catal., 30 (1985) 27.
[30] B.K. Teo et al., to be published.

[31] T.G.M.M. Kappen, P.P.J. Schlebos, J.J. Bour, W.P. Bosman, J.M.M. Smits, P.T. Buerskens and J.J. Steggerda, Inorg. Chem., 33 (1994) 754.
[32] (a) B.K. Teo, H. Dang and H. Zhang, to be published.
(b) B.K. Teo, X. Shi and H. Zhang, submitted for publication.
[33] G.A. Somorjai, Chemistry in Two Dimensions: Surfaces, Cornell University Press, Ithaca, NY, 1981.
[34] (a) R. Bouwman and W.M.H. Sachtler, J. Catal., 19 (1970) 127.
(b) J.H. Sinfelt, Acc. Chem. Res., 20 (1987) 134.
(c) F.L. Williams and M. Boudart, J. Catal., 30 (1973) 438.